Documenting drainage evolution in Bir Kiseiba, southern Egypt: Constraints from ground-penetrating radar and implications for Mars

John A. Grant, Ted A. Maxwell, and Andrew K. Johnston
Center for Earth and Planetary Studies, National Air and Space Museum, Smithsonian Institution, Washington, D. C., USA

Ali Kilani
Egypt Geological Survey and Mining Authority, Abbasiya, Cairo, Egypt

Kevin K. Williams
Center for Earth and Planetary Studies, National Air and Space Museum, Smithsonian Institution, Washington, D. C., USA

Received 29 December 2003; revised 26 May 2004; accepted 12 July 2004; published 1 September 2004.

[1] Ground-penetrating radar (GPR) helps to constrain the origin of relict and largely buried fluvial channels in the Bir Kiseiba region of southern Egypt. Our results indicate that the trunk channel to a tributary system identified in Shuttle Imaging Radar data is incised 10–12 m into bedrock, was southwest draining in its final configuration and laterally migrating toward the northwest, and accentuated relief along the nearby Kiseiba escarpment. Alluvium partially filling the main channel likely reflects effects of increasing aridity and bed load combined with less frequent, flashier precipitation. In contrast to defining channel margins, radar data do not indicate subtle stratigraphic changes in bedding related to fluvial aggradation, but do highlight local reflections likely corresponding to relict alluvial bedforms. Our results support the contention that an impulse GPR system, currently under development, could be deployed on a future Mars rover and assist in defining the regional evolution of the landscape and specific targets for sampling. *INDEX TERMS:* 5494 Planetology: Solid Surface Planets: Instruments and techniques; 5415 Planetology: Solid Surface Planets: Erosion and weathering; 5455 Planetology: Solid Surface Planets: Origin and evolution; 5470 Planetology: Solid Surface Planets: Surface materials and properties; *KEYWORDS:* GPR, Mars, Sahara

Citation: Grant, J. A., T. A. Maxwell, A. K. Johnston, A. Kilani, and K. K. Williams (2004), Documenting drainage evolution in Bir Kiseiba, southern Egypt: Constraints from ground-penetrating radar and implications for Mars, *J. Geophys. Res.*, *109*, E09002, doi:10.1029/2003JE002232.

1. Introduction

[2] The northeastern Sahara is the key area where the Space Shuttle Imaging Radar missions (SIR-A, B and C) documented the presence of subsurface channels beneath the active sand sheet [*McCauley et al.*, 1982; *Schaber et al.*, 1986; *Davis et al.*, 1993]. In the central part of the Selima Sand Sheet several sizes of channels were interpreted to represent Tertiary through Quaternary drainage patterns, consisting of trunk channels tens of kilometers wide to smaller superposed channels tens of meters across [*Haynes*, 1982]. Confirmation of a fluvial origin was based on extensive trenching with a backhoe, revealing distinctive sands and rounded gravels in the subsurface [*McCauley et al.*, 1982]. Data from the SIR-C mission has also revealed a distinct dendritic pattern of channels in the Kiseiba region, isolating a topographic surface with early Paleolithic artifacts [*Haynes et al.*, 1997], and forming a dendritic pattern in the lowest surface of the sand sheet [*Maxwell et al.*, 2002]. On the basis of the orbital radar data, the general nature of the channel system in the Kiseiba area is apparent, but little information can be gleaned regarding its depth, lithology, and stratification.

[3] In the field, we have found that the combination of shallow lag-covered swells in the sand sheet, near-surface bedrock, and certain types of sedimentary units all combine to create the light and dark dendritic pattern in the orbital SIR data. Although the fluvial pattern is distinctive, the cause for the individual radar reflections is not. Over several years, we have trenched, dug shallow test pits, and geometrically co-located Landsat, SPOT (Le Systeme Pour l'Observation de la Terre), and SIR-C data to determine the exact nature of the reflections. In order to confirm these data, we utilized ground-penetrating radar (GPR) in 2002 to determine the nature of the reflecting horizons in the subsurface, the depth of the paleochannels, whether subsurface stratification could be used to identify drainage direction, and to extend the results of 22 trenches used to determine local stratigraphic relations. The purpose of this paper is to document the new evidence for fluvial evolution of the paleochannels found using GPR and only hinted at with the

0148-0227/04/2003JE002232$09.00

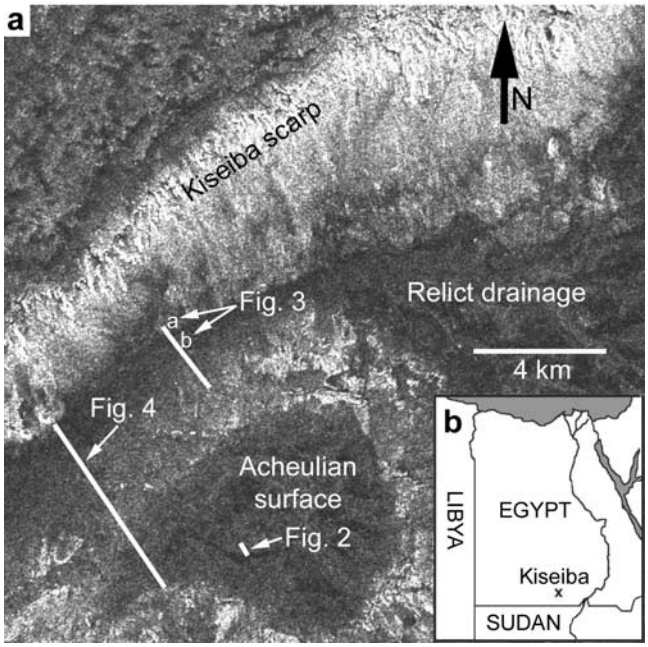

Figure 1. (a) Location of the study area in (b) the Bir Kiseiba region in southern Egypt. SIR-C radar map of the immediate study area (Figure 1a) created using L-minus-C band data (L and C radar bands are 24 cm and 5.7 cm in wavelength, respectively). North is toward the top of the figure, and selected GPR transects crossing the relict drainage are indicated, as are the specific locations of Figures 2–4 (arrows).

SIR-C data, and to evaluate the use of GPR in this Mars-like geomorphic environment, a hyperarid desert that was previously sculpted by fluvial processes.

2. Physical Setting

[4] The Bir Kiseiba region of southern Egypt is located in the Darb El Arba'in desert near 22.5°N, 30.5°E and is underlain by Quaternary surficial deposits and shale bedrock of the early Tertiary Dakhla Formation [*Issawi*, 1971]. The study area (Figure 1) lies below the southeast facing ~20 m Kiseiba Scarp and is characterized by a low-relief sand sheet that surrounds an inlier of an older Acheulian surface (evolved approximately 70,000 to 200,000 years before present [*Schild and Wendorf*, 1984; *Haynes et al.*, 1997]). Although depth to the water table is approximately 1 m at an oasis located 15 km to the west, the depth to the water table in the study area is unknown, but both GPR data and auguring to bedrock confirm that it is located more than 12 m below the surface. The sand sheet surface is characterized by coarse quartz sand and associated gravelly lag that caps a sequence of variably sandy, quartz pebble alluvial gravel [*Maxwell and Haynes*, 2001]. Local bedrock protrusions through the sand sheet are often capped by lags of Dakhla shale characterized by abundant diagenetic manganese that enhances resistance to weathering, whereas other locales are punctuated by low-density gypsum anhydrite deposits [*Maxwell et al.*, 2002].

[5] In the SIR-C "Data Take" of the region (DT-66.50; April, 1994) the Kiseiba scarp is the brightest reflector, resulting from the southwest looking radar reflected by the scoured bedrock of the scarp. Below the scarp to the southeast, sand sheet surfaces are separated from the scarp by a linear, radar-dark zone that branches into a dendritic pattern to the northeast. *Schild and Wendorf* [1984] first interpreted the basal sands of the linear zone southeast of the scarp to be fluvial deposits of early to middle Paleolithic age on the basis of three excavated archaeological sites. On the basis of the Shuttle radar data and associated field work, we have interpreted the dendritic pattern to represent a tributary system that fed the main channel against the scarp. GPR data have extended this interpretation, suggesting that the main channel is 12 m or more in depth, contains fluvial stratification, and

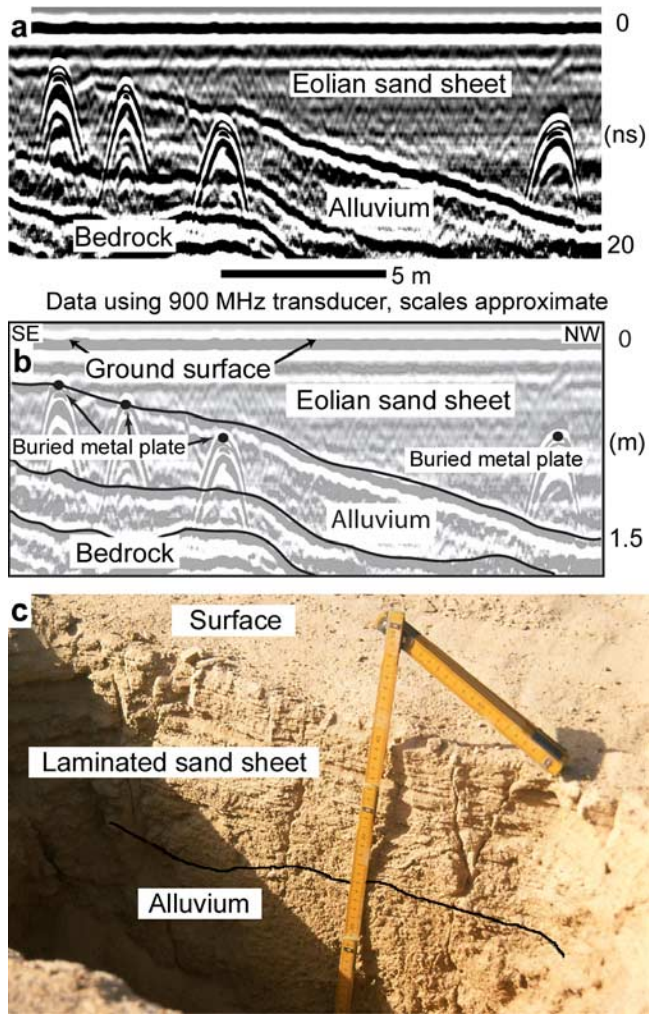

Figure 2. (a) GPR data and (b) interpretation highlighting reflections (white/black pairs) from metal plates buried in pits (hyperbolic reflections; east is to the left). Plates were buried to obtain ground truth used to help constrain the origin of various reflections that in this location correspond to a pedogenic carbonate layer (trending down to right along top of plate reflections) at the base of the sand sheet that overlies a thin layer of alluvium and in situ bedrock. Transect is from NW to SE from left to right. (c) Field photo of pit excavated along the transect described in Figure 2a that records the character of deposits comprising the eolian sand sheet and underlying alluvium. Metal plates were buried out of view in pit bottoms.

that the uppermost one to several meters of sediments are sand sheet, or sand sheet-derived, indicating later sedimentation unrelated to the original channel form.

3. Methods

[6] Ground-penetrating radar provides a rapid, nonintrusive means for characterizing the near-surface geology and structure to depths of 10–15 m [e.g., *Ulriksen*, 1982; *Paillou et al.*, 2001; *Grant et al.*, 2003]. Field work employed a GSSI SIR-20 GPR system configured with 400 MHz (75 cm wavelength) and 900 MHz (33 cm wavelength) antennas. Existing remote sensing (SIR and Landsat) and field data (Global Positioning System (GPS), sedimentological, and archeological) formed the basis for groundtruthing GPR transects that ranged in length from tens of meters to over 3 km.

[7] Three methods were used to characterize the radar properties of the subsurface. First, targets (metal plates) were buried along transects at depths up to ~2 m (Figure 2). Resultant data collected over and beside the refilled pit yielded no difference in appearance of the data and provided the means for field derivation of permittivity and for correlation between radar and the stratigraphy of the near-surface. A second method involved GPR data collection along transects undisturbed by excavation and predicting depth to interfaces using the experience gained from the first method. Predicted depths to reflections were generally within 10 cm of actual depth. Finally, field samples were sent in for laboratory derivation of permittivity and resulted in values similar to those derived in the field. The extremely low relief along the transects precludes the need for correction for topographic variations.

[8] Both the sand sheet and the underlying alluvium are characterized by a permittivity of 2.0 to 2.2, somewhat lower than the values reported by *McCauley et al.* [1982] for sediments in Wadi Arid 50 km to the west. Subtle stratigraphic variations in sand sheet units seen elsewhere [*Maxwell*, 1982; *Maxwell and Haynes*, 2001] are not distinguished in the GPR data due to the relatively invariant compositional properties combined with the small scale of the sand sheet units (several centimeters) as compared to the incident radar wavelengths. Radar distinction between the sand sheet and alluvium is typically unambiguous, however, due to some pedogenic alteration that enhances stratigraphic contacts, as well as local intraalluvial sedimentologic (e.g., gravel lenses) and pedogenic variability (Figure 3).

[9] Additional samples were also obtained and were used to constrain compositional and other physical properties. The surficial materials are extremely dry (less than 0.6% to

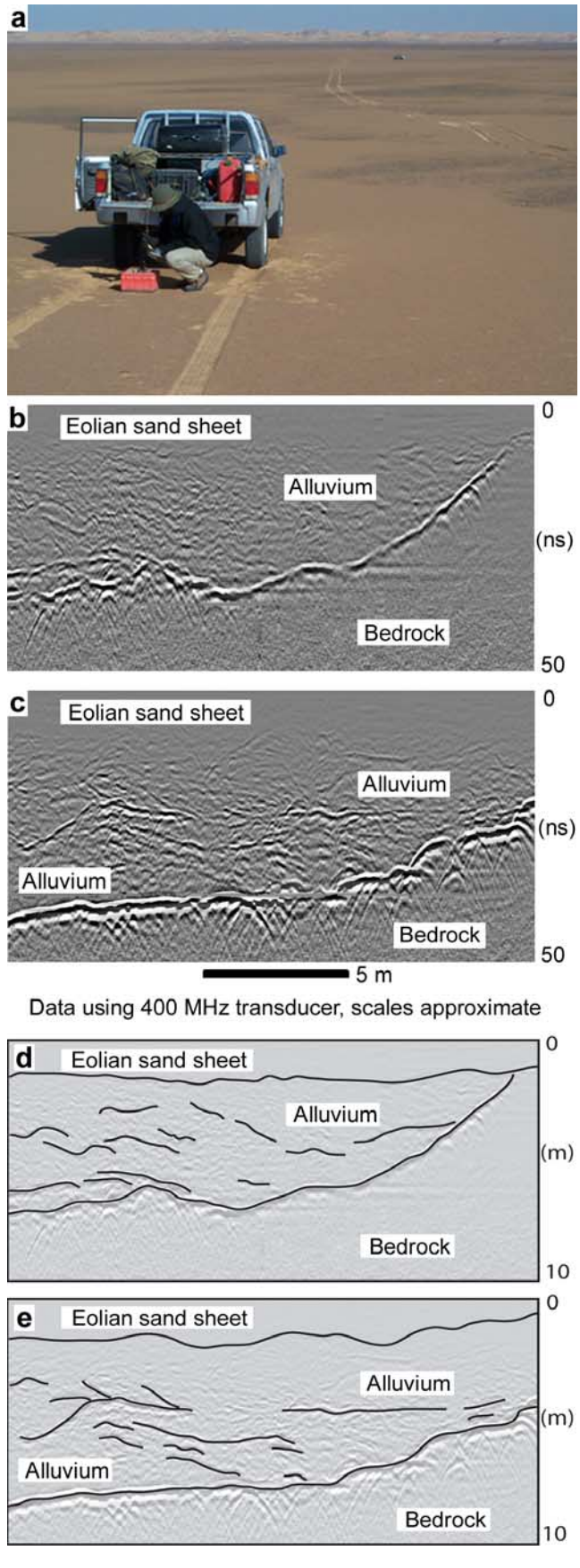

Figure 3. (a) Location of a GPR transect, (b and c) data, and (d and e) interpretation for a portion of the middle transect completed across the relict drainage (Figure 1). View in top is northwest toward Kiseiba scarp from flank of the Acheulian surface. The transect (Figure 3a) closely followed tracks toward truck in distance. Note relatively steep edge of channel in Figure 3b and discontinuous reflections characterizing the alluvium filling the channel (Figures 3b–3e). Northwest is to right of both (Figures 3b–3e). The total transect length was more than 1.5 km.

0.8% water by weight) and are predominantly quartz [*Schild and Wendorf*, 1984; *Maxwell et al.*, 2002]. The radar reflectivity of sediment interfaces between alluvial units is often accentuated by presence of some pedogenic hematite and/or carbonate. Although hematite coatings are locally present in the bulk sediments (mostly in the alluvium) they do not dominate [*El-Baz and Prestel*, 1982; *Maxwell*, 1982]. By contrast, laboratory analysis reveals that some local contacts are characterized by up to 1.6% to 2.7% hematite, mostly as amorphous grains. Similarly, laboratory analysis reveals that pedogenic carbonate along some contacts increases locally to a maximum measured 28% by weight.

4. Radar Stratigraphy

[10] Excellent radar penetration was achieved along many transects and ranged generally between 2 and 4 m with the 900 MHz antenna and 10–12 m with the 400 MHz antenna. These penetration depths apparently exceed those realized by *Paillou et al.* [2003] for locations in the Safsaf region to the west. Exceptions to the penetration depths realized in the Bir Kiseba region were noted in areas characterized by anhydrite deposits and the manganiferous shale, either in situ or as lags, where minimal penetration was achieved.

[11] Data from GPR transects completed across the trunk channel (Figure 1) generally permit tracing the entire cross-section and indicates that the maximum depth is 10–12 m below the present surface (Figure 3). Margins of the channel closely correspond to shallow outcroppings of bedrock as confirmed by excavation. Hence the channel is incised entirely into bedrock.

[12] Review of the GPR data reveals the trunk channel was migrating laterally to the northwest. Support for this statement is in the form of a relatively steep northwest channel flank (Figure 3b) such as is commonly associated with a laterally eroding cutbank [*Ritter et al.*, 1995]. In addition, there are multiple northwest dipping reflections along the southeast channel margin that pinch out along the channel floor (Figure 4); these are best interpreted as alluvial wedges accreted along a northwest migrating channel. The northerly dip of the fluvial sands beneath the sand sheet and alluvium is consistent with the orientation of bedding seen in the trenches excavated by Schild and Wendorf in 1979 [*Schild and Wendorf*, 1984].

[13] In contrast to the sand sheet, alluvium within the channel is marked by numerous discontinuous horizontal to variably dipping reflections that are typically 5–10 m across and display 1–2 m of relief (Figure 3). These reflections are noted in the main channel and in apparent tributary channels farther to the east. Whereas the depth and scale of these features precludes complete excavation, comparison with sediments outcropping in pits implies that the reflections correspond to variability in gravel versus sand content in the alluvium. The signature of these grain-size differences may be enhanced by pedogenic alteration (e.g., local carbonate and/or hematite deposition). The scale and distribution of these radar features combined with the observed variability in the alluvium suggests that they are depositional bedforms partially filling the channel [e.g., *Leeder*, 1982].

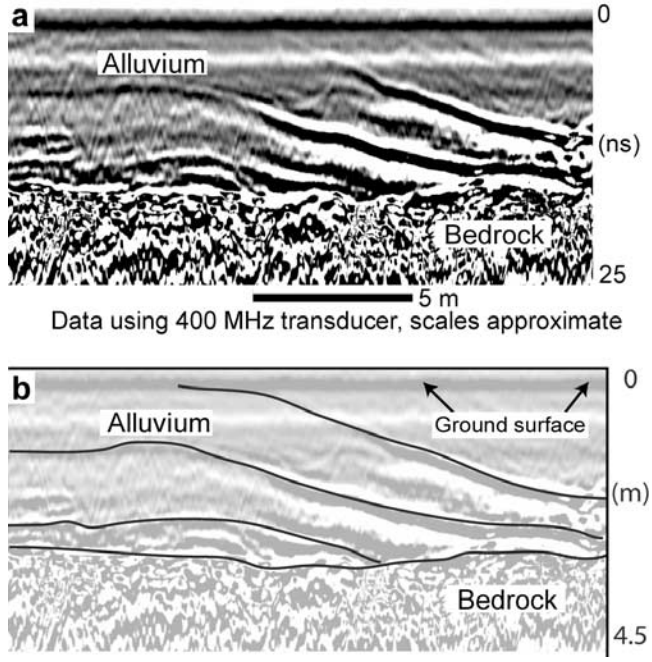

Figure 4. (a) GPR data and (b) interpretation from a portion of the westernmost transect across the relict channel (Figure 1). Total transect was ~2.8 km long and followed a series of large pits excavated by a backhoe during a prior field season that were used for ground truth. Series of dipping reflections most likely correspond to alluvial wedges accreted as the channel migrated laterally toward the northwest (toward the right side of Figures 4a and 4b).

[14] Finally, stratigraphic control from numerous trenches up to 3 m deep indicates subtle cross-stratified gravel lenses, and textural variations between stratified and featureless sand deposits are apparent but are not detectable in the GPR data. These results are likely due to the long wavelength of the GPR relative to the scale of the gravel lenses (several centimeters thick). Nevertheless, the GPR data confirm that the bedrock surface is undulating at depths generally less than those noted for transects crossing the trunk channel to the west.

5. Drainage Evolution

[15] GPR data provide a glimpse of an ancient fluvial landscape evolving under conditions that were much different from the hyperarid climate that currently characterizes the region. Regional drainage was responsible for downcutting a bedrock channel that was migrating laterally to the northwest, isolating the Acheulian surface [*Haynes et al.*, 1997], and accentuating relief associated with the Kiseiba scarp. The resultant fluvial signature, although subsequently modified by eolian processes, continues to dominate the local geologic setting.

[16] On the basis of the apparent northerly dip of the basal sands seen in their archeological trenches, *Schild and Wendorf* [1984] interpreted the earliest drainage of the Kiseiba depression as flowing to the northeast. However, on the basis of junction angles between tributaries and the trunk channel [*Ritter et al.*, 1995] that are deduced from SIR

images (Figure 1), as well as the increased incision that might be expected downstream, it is equally plausible that the channel drained to the southwest. Interpretation of GPR data obtained across the trunk channel and locations to the east indicates that while the depth of the channel thalweg varies little and may even shallow by ~1–2 m in a southwesterly direction, the depth to bedrock shallows considerably to the east. Hence we conclude that the drainage was to the southwest, consistent with the observed overall depth of incision and to bedrock.

[17] The key to the paleodrainage direction is whether the complex digitate network northeast of the GPR sections shown here (Figure 1) is a tributary or distributary system, and how the present channel fill relates to the original fluvial environment. Postfluvial eolian erosion of the evolved landscape also plays an important role in defining measured channel depth. Differential GPS measurements of topography completed along the cross-channel transects (Figure 1) indicate that there is up to 5 m of broadly undulating relief along the surface presently burying the channels. This relief currently precludes continuous drainage in any direction and in the absence of tectonics likely reflects eolian erosion of the variably resistant surface and associated eolian deposits. For example, deflation is less efficient where fluvial lags are best developed [*Maxwell et al.*, 2002, 2003]. Hence the local setting is characterized by up to 5 m of eolian erosion and/or deposition that contributes to observed variations in channel depth and the poorly integrated nature of the present surface.

[18] Channel incision into bedrock indicates at least portions of the downcutting history were characterized by sufficient stream power to enable transport of bed load without long term storage within the channel. Such discharge characteristics are consistent with channel incision occurring under wetter-than-present conditions. The lack of coarse material derived from the adjacent Kiseiba scarp in the near surface sediments indicates that at least the terminal stages of fluvial aggradation resulted in sediments derived from a fine-grained source, consistent with southward drainage and material derived from the alluvial plain to the north. The presence of significant alluvium near the top of the sections indicates that active fluvial sedimentation changed prior to inactivity as a result of increasing aridity as vegetation cover decreased and discharge became less regular and increasingly flashy. It is therefore likely that the fluvial system in the Bir Kiseiba region records a transition from an actively incising system capable of transporting the introduced sediment load to one characterized by sediment storage within the channel, thereby resulting in aggradation as stream power was expended. Prior to becoming inactive, the channel most likely had become braided and characterized by intermittent discharge. Once inactive, the channel was reshaped by eolian processes that deranged the regional drainage system. As a result, infrequent precipitation now leads to localized ponding and deposition of evaporites in small playas flanking what was once an active channel.

6. Comparisons to SIR Data

[19] The conclusions from the GPR study of the Bir Kiseiba region allow us to extend the interpretations drawn from the SIR data of the region, providing significant additional clues to the evolution of the relict fluvial landscape, as a result of increased penetration and higher spatial resolution. Indeed, GPR definition of areally extensive reflections at depths of 1.5–2 m that go largely undetected in the SIR data support the earlier conclusion [e.g., *McCauley et al.*, 1982; *Schaber et al.*, 1986; *Paillou et al.*, 2003] that SIR penetration and detection of subsurface reflections was generally limited to 1–2 m. The complementary nature of the GPR, SIR, and field data sets enables definition of both surface and subsurface characteristics of the ancient fluvial landforms, which demonstrate that the current hyperarid eolian environment does little to mask the ancient fluvial landscape except in the nearest surface sediments.

7. Implications for Mars

[20] The Egyptian study area occurs within a portion of the Sahara Desert that has long been considered to possess potential analogs for landforms on Mars [e.g., *Maxwell and El-Baz*, 1982; *Garvin*, 1982; *Paillou et al.*, 2001]. Although the mineralogical setting in Egypt is not likely a good Mars analog, the minimal contrast across geomorphic boundaries is offset by extremely dry conditions and yields distinct reflections to significant depths (Figures 2–4). Similar radar contrasts across geomorphic boundaries may be reasonable to expect on Mars in spite of differing compositional properties and given the expectation of extremely dry conditions. Hence our results from Egypt combined with consideration of factors influencing radar performance on Mars instill confidence that a rover-deployed GPR can assist in defining geologic setting on that planet.

[21] For example, low ambient temperature and a dry near-surface on Mars should mitigate difficulties related to the presence of any fines or salts [*Collins and Kurtz*, 1998; *Malin et al.*, 1998]. Although dielectric values of 3–10 likely characterize the near-surface [*Simpson et al.*, 1992; *Muhleman*, 1995; *Barbin et al.*, 1995], corresponding loss tangents are less understood [*Leuschen et al.*, 2001], but are likely 0.05 to 0.1 and may be locally as high as ~0.3 [*Heggy et al.*, 2003]. Such losses might limit deep radar penetration to ~10 times the wavelength [*Simpson et al.*, 1992] or approximately 7.5 to 20 m for a GPR operating between 150 MHz and 400 MHz. Magnetic losses may also be locally or regionally important in substrates with significant iron-bearing minerals [*Olheoft*, 1998; *Paillou et al.*, 2001] and can be avoided via careful landing site selection.

[22] A rover-deployable impulse GPR currently under development for future Mars missions [*Grant et al.*, 2003] should possess instrument capabilities comparable to those achieved in Egypt. The system controller is low mass, volume, and power with expected limits of 0.5 kg, 3400 cm^3, 3 W (peak), respectively. Moreover, the GPR will possess few or no moving parts, may include a body conformal antenna capable of configuration at ~150 MHz to more than 600 MHz, collect ~0.3 MB/day (assuming a 50 m traverse) [*Grant et al.*, 2003], and is being successfully tested in Mars analog environments (Figure 5).

[23] By analogy to the results from Bir Kiseiba, a Mars GPR deployed in the vicinity of valley networks should be able to distinguish geomorphic signatures of a comparable scale. Although the mineralogical setting on Mars will differ,

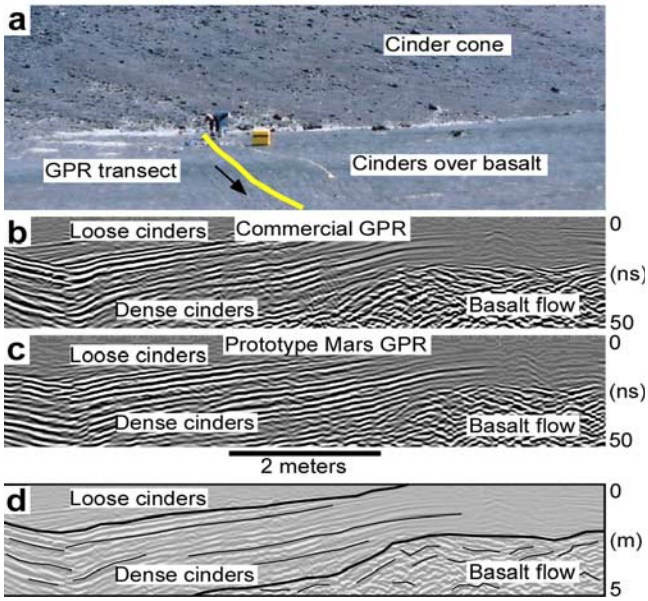

Figure 5. (a) GPR data with interpretation from layered, alternating loose and dense iron-rich cinders overlying the Bonito a'a lava flow at Sunset Crater, Arizona, that demonstrates the utility of GPR in such environments which may be compositional analogs for some locations on Mars. Data collected along a transect crossing the cinder deposits (Figure 5a) using (b) a commercial GPR and 400 MHz antenna and (c) prototype Mars high-frequency 600 MHz antenna deployed ~15 cm above ground that leads to (d) similar interpretation of stratigraphy. Both the commercial and prototype data were processed using a horizontal IIR filter run at a low-pass setting of 50 scans and a high pass setting of 5 scans.

the relative scale and geometry of stratigraphy in alluvial/fluvial settings should approximate that observed in terrestrial environments. Hence the stratigraphic variability responsible for creating dielectric contrasts in Egypt may also occur on Mars. The ready detection of radar reflections in Egypt where minimal mineralogical contrasts are present bodes well for Mars where mineralogical variability may be different but similarly subtle and suggests the capability for denoting reflections whose geometry may be diagnostic of the source and persistence of water responsible for formation.

[24] Deployment near valley heads and detection of buried incipient tributaries on Mars such as was possible in Egypt would support formation by precipitation-induced runoff, whereas definition of relict piping or seepage features would be more indicative of an origin by groundwater sapping. The character of intravalley channels and deposits (e.g., bedrock channels versus alluvial bars versus eolian) could assist in understanding the transition from a fluvial to predominantly an eolian geomorphic system. In addition to high science potential, a Mars impulse GPR could assist the rover in detecting and avoiding hazards (e.g., dust-filled cracks or voids such as those encountered by the Mars Exploration Rover Opportunity in Meridiani Planum [*Squyres and the Athena Science Team*, 2004]).

[25] Given these performance attributes, we conclude that a GPR on Mars could assist in defining geologic setting, identify diagnostic signatures required for distinguishing the sources of water responsible for shaping the ancient Martian landscape, and provide critical guidance for collecting samples for in situ analyses and/or sample return to the Earth.

8. Conclusions

[26] Ground-penetrating radar defines reflections associated with a relict and largely buried fluvial system in the Bir Kiseiba region of southern Egypt that produced a landscape that continues to dominate the local geology. Ground truth together with the geometry of the reflections allow conclusions to be drawn regarding the evolution of the system, which includes bedrock incision to at least 10–12 m depth in a northwest migrating channel that was accentuating topography along the nearby Kiseiba scarp. Subsequent alluvial aggradation within what was likely a southwest draining channel marked a transition to more arid conditions characterized by eolian redistribution of materials that partially masked and deranged the drainage pattern via up to 5 m of vertical erosion and/or local deposition.

[27] Subtle laminations of sand sheet strata are not visible in GPR at 400 MHz, nor are thin gravel stringers diagnostic of fluvial sediments. In contrast, however, GPR does an excellent job of delineating the margins and bottoms of former channels due to the density and lithology contrast at the base of the channels. Such data are complementary to the SIR and field data and permit the evolution of this enigmatic landscape to be better understood.

[28] Finally, GPR deployment in Mars-analog settings such as Egypt (from a geomorphic perspective) provides an opportunity to explore the potential utility of an instrument currently under development for possible future rover-deployment on Mars. Based the quality of data obtained in Egypt, we conclude that a GPR on Mars could define radar stratigraphy of similar scale and complexity to depths of ~10−15 m, thereby helping to define geologic setting and provide critical context necessary for targeting (rover positioning) and interpreting results from other sampling and in situ instrumentation.

[29] **Acknowledgments.** We thank Ilya Buynevich, Jeff Plescia, and an anonymous reviewer for comments that resulted in a significantly improved manuscript. Thanks also to Ross Irwin and Corey Fortezzo for help with the figures and formatting. Work was supported by The Becker Endowment of the Smithsonian and NASA PIDDP grant NAG5-10256.

References

Barbin, Y., F. Nicollin, W. Kofman, V. Zolotarev, and V. Glotov (1995), Mars 96 GPR program, *J. Appl. Geophys.*, *33*, 27–37.

Collins, M. E., and J. L. Kurtz (1998), Assessing GPR performance in three soil geographic regions, paper presented at GPR '98: Seventh International Conference on Ground-Penetrating Radar, Univ. of Kansas, Lawrence.

Davis, P. A., C. S. Breed, J. F. McCauley, and G. G. Schaber (1993), Surficial geology of the Safsaf Region, south-Central Egypt, derived from remote-sensing and field data, *Remote Sens. Environ.*, *46*, 183–203.

El-Baz, F., and D. Prestel (1982), Coatings on sand grains from southwestern Egypt, in *Desert Landforms of Southwest Egypt: A Basis for Comparison With Mars*, *NASA CR-3611*, edited by F. El-Baz and T. A. Maxwell, pp. 175–188, U.S. Govt. Print. Off., Washington, D. C.

Garvin, J. B. (1982), Characteristics of rock populations in the western desert and comparison with Mars, in *Desert Landforms of Southwest Egypt: A Basis for Comparison With Mars*, *NASA CR-3611*, edited by F. El-Baz and T. A. Maxwell, pp. 261–280, U.S. Govt. Print. Off., Washington, D. C.

Grant, J. A., A. E. Schutz, and B. A. Campbell (2003), Ground-penetrating radar as a tool for probing the shallow subsurface of Mars, *J. Geophys. Res.*, *108*(E4), 8024, doi:10.1029/2002JE001856.

Haynes, C. V., Jr. (1982), The Darb El Arba'in Desert: A product of Quaternary climate change, in *Desert Landforms of Southwest Egypt: A Basis for Comparison With Mars*, *NASA CR-3611*, edited by F. El-Baz and T. A. Maxwell, pp. 91–117, U.S. Govt. Print. Off., Washington, D. C.

Haynes, C. V., Jr., T. A. Maxwell, A. El-Hawary, K. A. Nicoll, and S. Stokes (1997), An Acheulian site near Bir Kiseiba in the Darb el Arba'in Desert, Egypt, *Geoarchaeology*, *12*, 819–832.

Heggy, E., P. Paillou, F. Costard, N. Mangold, G. Ruffie, F. Demontoux, G. Grandjean, and J. M. Malézieux (2003), Local geoelectrical models of the Martian subsurface for shallow groundwater detection using sounding radars, *J. Geophys. Res.*, *108*(E4), 8030, doi:10.1029/2002JE001871.

Issawi, B. (1971), Geology of the Darb El Arba'in, Western Desert, *Ann. Geol. Surv. Egypt*, *1*, 53–92.

Leeder, M. R. (1982), *Sedimentology: Process and Product*, 344 pp., Allen and Unwin, Concord, Mass.

Leuschen, C. J., S. P. Gogineni, S. M. Clifford, and R. K. Raney (2001), Design of a ground-penetrating radar for Mars, in *Abstracts From the Conference on the Geophysical Detection of Subsurface Water on Mars*, edited by S. Clifford, J. George, and C. Stoker, *LPI Contrib. 1095*, pp. 64–65, Lunar and Planet. Inst., Houston, Tex.

Malin, M. C., et al. (1998), Early views of the Martian surface from the Mars Orbiter Camera of Mars Global Surveyor, *Science*, *279*, 1681–1685.

Maxwell, T. A. (1982), Sand sheet and lag deposits in the Southwestern Desert, in *Desert Landforms of Southwest Egypt: A Basis for Comparison With Mars*, *NASA CR-3611*, edited by F. El-Baz and T. A. Maxwell, pp. 157–174, U.S. Govt. Print. Off., Washington, D. C.

Maxwell, T. A., and F. El-Baz (1982), Analogs of Martian eolian features in the western desert of Egypt, in *Desert Landforms of Southwest Egypt: A Basis for Comparison With Mars*, *NASA CR-3611*, edited by F. El-Baz and T. A. Maxwell, pp. 247–260, U.S. Govt. Print. Off., Washington, D. C.

Maxwell, T. A., and C. V. Haynes Jr. (2001), Sand sheet dynamics and Quaternary landscape evolution of the Selima sand sheet, southern Egypt, *Quat. Sci. Rev.*, *20*, 1623–1647.

Maxwell, T. A., J. A. Grant, A. Johnston, and B. A. Campbell (2002), Use of orbital and ground-penetrating radar to understand climate change on Earth and Mars, *Geol. Soc. Am. Abstr. Programs*, *34*, 174.

Maxwell, T. A., J. A. Grant, B. A. Campbell, R. P. Irwin III, M. Bourke, and A. Johnston (2003), Erasure of first-order tributaries via climate change: Lessons for Mars from Earth, *Proc. Lunar Planet. Sci. Conf. 34th*, abstract 2049.

McCauley, J. F., G. G. Schaber, C. S. Breed, M. J. Grolier, C. V. Haynes, B. Asissawi, C. Elachi, and R. Blom (1982), Subsurface valleys and geoarcheology of the eastern Sahara revealed by Shuttle Radar, *Science*, *218*, 1004–1020.

Muhleman, D. O. (1995), Radar observations of Mars, Mercury, and Titan, *Annu. Rev. Earth Planet. Sci.*, *23*, 337–374.

Olheoft, G. R. (1998), Electrical, magnetic, and geometric properties that determine ground penetrating radar performance, paper presented at GPR '98: Seventh International Conference on Ground-Penetrating Radar, Univ. of Kansas, Lawrence.

Paillou, P., G. Grandjean, J. M. Malezieux, G. Ruffie, E. Heggy, D. Piponnier, P. Dubois, and J. Achache (2001), Performances of ground penetrating radars in arid volcanic regions: Consequences for Mars subsurface exploration, *Geophys. Res. Lett.*, *28*, 911–914.

Paillou, P., G. Grandjean, N. Baghdadi, E. Heggy, T. August-Bernex, and J. Achache (2003), Subsurface imaging in South-central Egypt using low-frequency radar: Bir Safsaf revisited, *IEEE Trans. Geosci. Remote Sens.*, *41*, 1672–1684.

Ritter, D. F., R. C. Kochel, and J. R. Miller (1995), *Process Geomorphology*, 540 pp., Brown, Dubuque, Iowa.

Schaber, G. G., J. F. McCauley, C. S. Breed, and G. R. Olhoeft (1986), Shuttle imaging radar: Physical controls on signal penetrating and subsurface scattering in the eastern Sahara, *IEEE Trans. Geosci. Remote Sens.*, *GE-24*, 603–623.

Schild, R., and F. Wendorf (1984), Lithostratigraphy of Holocene lakes along the Kiseiba scarp, in *Cattle-Keepers of the Eastern Sahara: The Neolithic of Bir Kiseiba, assembled by F. Wendorf and R. Schild*, edited by A. E. Close, pp. 9–40, Southern Methodist Univ. Press, Dallas, Tex.

Simpson, R. A., J. K. Harmon, S. H. Zisk, T. W. Thompson, and D. O. Muhleman (1992), Radar determination of Mars surface properties, in *Mars*, edited by H. H. Kieffer et al., pp. 652–685, Univ. of Ariz. Press, Tucson.

Squyres, S., and the Athena Science Team (2004), Initial results from the MER Athena Science Investigation at Gusev Crater and Meridiani Planum, *Eos Trans. AGU*, *85*(17), Jt. Assem. Suppl., Abstract U43A-01.

Ulriksen, C. P. F. (1982), Application of impulse radar to civil engineering, Ph.D. thesis, 175 pp., Univ. of Technol., Lund, Sweden.

J. A. Grant, A. K. Johnston, T. A. Maxwell, and K. K. Williams, Center for Earth and Planetary Studies, National Air and Space Museum, Smithsonian Institution, 6th Street at Independence Avenue, SW, Washington, DC 20560-0315, USA. (grantj@nasm.si.edu)

A. Kilani, Egypt Geological Survey and Mining Authority, Abbasiya, Cairo, Egypt.